Accepted Manuscript

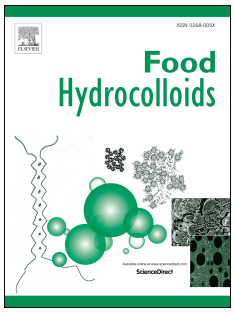

Relationships between amylopectin molecular structures and functional properties of different-sized fractions of normal and high-amylose maize starches

Lingshang Lin, Canhui Cai, Robert G. Gilbert, Enpeng Li, Juan Wang, Cunxu Wei

PII: S0268-005X(15)30029-1

DOI: 10.1016/j.foodhyd.2015.07.019

Reference: FOOHYD 3075

To appear in: *Food Hydrocolloids*

Received Date: 4 March 2015

Revised Date: 9 June 2015

Accepted Date: 17 July 2015

Please cite this article as: Lin, L., Cai, C., Gilbert, R.G., Li, E., Wang, J., Wei, C., Relationships between amylopectin molecular structures and functional properties of different-sized fractions of normal and high-amylose maize starches, *Food Hydrocolloids* (2015), doi: 10.1016/j.foodhyd.2015.07.019.

Relationships between amylopectin molecular structures and functional properties of different-sized fractions of normal and high-amylose maize starches

Lingshang Lin[a,1], Canhui Cai[a,1], Robert G. Gilbert[b,c], Enpeng Li[b], Juan Wang[a], Cunxu Wei[a,*]

[a] Jiangsu Key Laboratory of Crop Genetics and Physiology/Co-Innovation Center for Modern Production Technology of Grain Crops, Yangzhou University, Yangzhou 225009, China

[b] Tongji School of Pharmacy, Huazhong University of Science and Technology, Wuhan 430030, China

[c] The University of Queensland, Centre for Nutrition and Food Sciences, Queensland Alliance for Agricultural and Food Innovation, Brisbane, QLD 4072, Australia

[1] These authors contributed equally to this work.

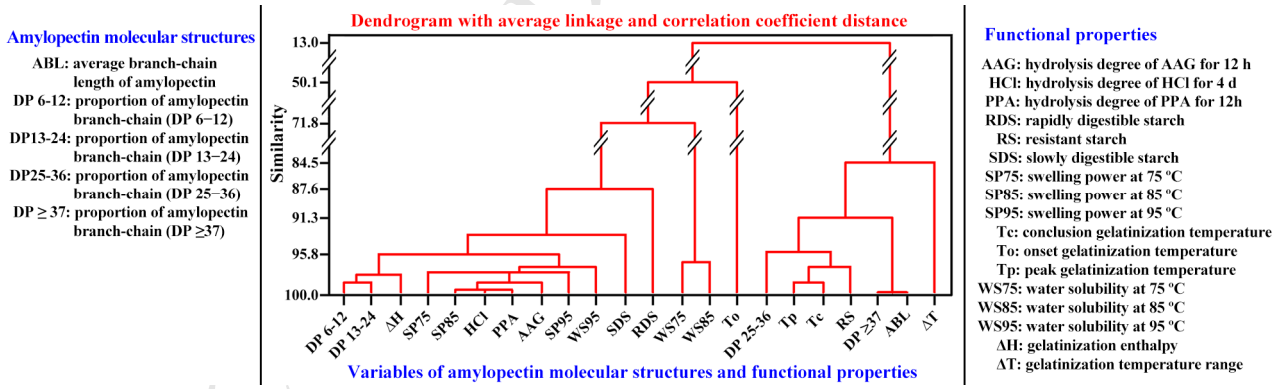

Graphical abstract

Relationships between amylopectin molecular structures and functional properties of different-sized fractions of normal and high-amylose maize starches

Lingshang Lin[a,1], Canhui Cai[a,1], Robert G. Gilbert[b,c], Enpeng Li[b], Juan Wang[a], Cunxu Wei[a,*]

[a] Jiangsu Key Laboratory of Crop Genetics and Physiology/Co-Innovation Center for Modern Production Technology of Grain Crops, Yangzhou University, Yangzhou 225009, China

[b] Tongji School of Pharmacy, Huazhong University of Science and Technology, Wuhan 430030, China

[c] The University of Queensland, Centre for Nutrition and Food Sciences, Queensland Alliance for Agricultural and Food Innovation, Brisbane, QLD 4072, Australia

[1] These authors contributed equally to this work.

* **Corresponding Author**

Cunxu Wei

Address: College of Bioscience and Biotechnology, Yangzhou University, Yangzhou 225009, China. Tel.: +86 514 87997217. Fax.: +86 514 87971747. E-mail: cxwei@yzu.edu.cn

Abbreviations

AAG: *Aspergillus niger* amyloglucosidase; DP: degree of polymerization; DSC: differential scanning calorimetry; FACE: fluorophore-assisted capillary electrophoresis; PPA: porcine pancreatic α-amylase; RDS: rapidly digestible starch; RS: resistant starch; SDS: slowly digestible starch.

Abstract

The amylopectin molecular structures and functional properties of different-sized fractions of normal and high-amylose maize starches were investigated and compared in this study. The different-sized fractions of normal starch showed similar amylopectin molecular structures and functional properties. The small-sized fraction of high-amylose starch had significantly higher amylopectin long branch-chain and average branch-chain length than its counterpart medium- and large-sized fractions. The swelling power, gelatinization enthalpy, and hydrolysis and digestion degrees of high-amylose starch significantly decreased with decrease of granule size, and were significantly positively correlated with amylopectin short branch-chain and negatively correlated with amylopectin long branch-chain and average branch-chain length. The gelatinization peak temperature and resistant starch content increased with decrease of granule size, and were significantly positively correlated with amylopectin long branch-chain and average branch-chain length and negatively correlated with amylopectin short branch-chain. The hierarchical cluster analysis indicated that the large-sized fraction of high-amylose starch was significantly different from the medium- and small-sized fractions of high-amylose starch but more relative with normal starch. The above results could provide important information for the applications of different-sized fractions of high-amylose maize starch.

Keywords: Normal maize starch; High-amylose maize starch; Starch granule size; Amylopectin molecular structure; Functional properties.

1. Introduction

In higher plants, starch consists of two main components, mainly linear amylose and highly branched amylopectin, and exists as discrete semicrystalline granules with varying sizes (1–100 μm), shapes (spherical, lenticular, polyhedral, and irregular), and size distributions (unimodal and bimodal) (Jane, Kasemsuwan, Leas, Zobel, & Robyt, 1994; Tester, Karkalas, & Qi, 2004a). Amylose content greatly influences the physicochemical and functional properties of starch. Starch with high amylose content has a high resistance to digestion and provides many health benefits for humans (Carciofi et al., 2012; Man et al., 2012; Regina et al., 2006; Slade et al., 2012; Zhu et al., 2012). Therefore, high-amylose starches are of interest because of their potential health benefits. Many high-amylose cereal varieties have been developed via mutation or transgenic breeding approaches (Carciofi et al., 2012; Regina et al., 2006; Slade et al., 2012; Zhu et al., 2012).

For starches with a bimodal size distribution such as wheat and barley, the large A-type starch has higher amylose content, lamellar repeat distance, gelatinization enthalpy and pasting viscosity, and lower amylopectin short branch-chain, gelatinization temperature, and swelling power than the small B-type starch (Li et al., 2013; Naguleswaran, Li, Vasanthan, Bressler, & Hoover, 2012; Salman et al., 2009; Takeda, Takeda, Mizukami, & Hanashiro, 1999; Tang, Ando, Watanabe, Takeda, & Mitsunaga, 2001). The different structural and functional properties result in the different end uses. For example, the starch with predominantly small B-type starch can be used as a fat substitute, a paper coating, and a carrier material in cosmetics, while the starch with a high percentage of large A-type starch has applications in the manufacture of biodegradable plastic film, carbonless copy paper, and

brewing beer (Lindeboom, Chang, & Tyler, 2004). For starches with a unimodal size distribution such as maize and potato, the amylose content and pasting viscosity increase and the gelatinization temperature and hydrolysis degree decrease with increasing granule size (Dhital, Shrestha, & Gidley, 2010; Dhital, Shrestha, Hasjim, & Gidley, 2011; Kaur, Singh, McCarthy, & Singh, 2007). The structural and functional property studies of different size granules can provide insights into the role that granule size plays in determining functional properties and uses of starches (Dhital et al., 2011). However, these studies are mainly focused on waxy and normal crop starches, particularly bimodal starches. Less work has been done to relate the effect of granule size to structural and functional properties in high-amylose starches. This might be due to the practical difficulty of separating different size granules from high-amylose starches.

Cereal endosperm starch granules with high-amylose content always show markedly different morphology and granule size (Cai, Huang et al., 2014; Cai, Lin et al., 2014; Cai, Zhao, Huang, Chen, & Wei, 2014; Carciofi et al., 2012; Man et al., 2014; Regina et al., 2006; Slade et al., 2012). Usually the granule size decreases with increase of amylose content in high-amylose crops (Cai, Huang et al., 2014; Cai, Lin et al., 2014; Cai, Zhao et al., 2014; Man et al., 2014). Recently, the different morphology and size starch granules in high-amylose cereal crops have been reported to have significantly different structure (Cai, Huang et al., 2014; Cai, Lin et al., 2014; Cai, Zhao et al., 2014; Dhital, Butardo, Jobling, & Gidley, 2015; Man et al., 2014). For example, the elongated granule has higher amylose content and amylopectin long branch-chain and lower amylopectin short branch-chain and branching degree than aggregate and individual granule in high-amylose maize (Cai, Lin et al., 2014;

Cai, Zhao et al., 2014). The amylose content, amylopectin long branch-chain, and short-range ordered degree significantly increase with decrease of granule size in high-amylose maize starch, but the amylopectin short branch-chain and branching degree, relative crystallinity, and lamellar peak intensity markedly decrease with decrease of granule size (Cai, Lin et al., 2014; Cai, Zhao et al., 2014). The interior hollow granule has very high amylose content and show amorphous structure (Cai, Huang et al., 2014; Man et al., 2014). However, the functional properties of different morphology and size granules have seldom been reported in high-amylose starches.

In our previous report, the large-, medium-, and small-sized fractions were separated from normal and high-amylose maize starches. The structural properties were similar among the different-sized fractions of normal starch, but markedly different among the different-sized fractions of high-amylose starch. The amylopectin long branch-chain, amylose content, and short-range ordered degree significantly increased, but the amylopectin short branch-chain and branching degree, relative crystallinity, and lamellar scattering peak intensity decreased with decreasing granule size of high-amylose maize starch. The large-, medium- and small-sized fractions of high-amylose maize starch were A-, C_A- and C-type crystallinity, respectively, indicating that B-type allomorph increased with decrease of granule size (Cai, Lin et al., 2014). However, their amylopectin molecular structures are unclear. For the applications of starch, it is necessary to investigate the functional properties including swelling power, water solubility, thermal property, hydrolysis property, digestion property, etc. As a follow-up study of the previous paper (Cai, Lin et al., 2014), we further investigated and compared the amylopectin molecular structures and some functional properties of

different-sized fractions of normal and high-amylose maize starches. The hierarchical cluster analysis of native and different-sized fractions of normal and high-amylose maize starches had also been constructed based on their amylopectin molecular structures and functional properties. The objective of this study was to analyze the relationships between amylopectin molecular structures and functional properties and investigate the hierarchical cluster of native and different-sized fractions of normal and high-amylose maize starches.

2. Materials and methods

2.1. Plant materials

Normal maize starch (S4126) (NS) and high-amylose maize starch (S4180) (HS) were purchased from Sigma-Aldrich. The apparent amylose contents determined by the iodine colorimetric method were about 31% and 56% for normal and high-amylose maize starches, respectively (Cai, Lin et al., 2014).

2.2. Separation of large-, medium-, and small-sized fractions

The normal and high-amylose maize starches were separated into large-, medium-, and small-sized fractions using glycerol centrifugation as described by Cai, Lin et al. (2014). Briefly, 40 mL of starch suspension (2.5%, w/v) in 80% glycerol was centrifuged at 100 *g* for 5 min. The supernatant was removed to a beaker. The pellet was suspended with 40 mL of 80% glycerol and centrifuged five times to obtain starch precipitate that constituted the large-sized fraction. The supernatants were pooled and centrifuged at 5000 *g* for 10 min. The resulting starch pellet was suspended with 40 mL of 60% glycerol and centrifuged at 100 *g* for 5 min. The supernatant was removed to a beaker. The pellet was suspended with 40 mL of 60% glycerol and centrifuged five times to obtain starch precipitate that constituted the

medium-sized fraction. The supernatants were pooled and centrifuged at 5000 *g* for 10 min. The resulting starch pellet comprised the small-sized fraction. Finally, the starch fractions were washed in distilled water and in anhydrous ethanol, and then dried at 40 °C for 2 days, ground into powders in a mortar with pestle, and passed through a 100-mesh sieve. The large-, medium-, and small-sized fractions had the volume-weighted mean diameter of 18.4, 14.5 and 9.0 μm for normal maize and 20.5, 14.4 and 8.5 μm for high-amylose maize, the apparent amylose content of 31.9, 31.2 and 29.7% for normal maize and 33.2, 50.5 and 74.1% for high-amylose maize, and the yield percentage of 10.7, 79.9 and 9.4% for normal maize and 9.6, 67.7 and 22.7% for high-amylose maize (Cai, Lin et al., 2014).

2.3. Fluorophore-assisted capillary electrophoresis (FACE) analysis

Starch was deproteinized with protease and sodium bisulfite, and debranched with isoamylase according to the methods of Tran et al. (2011) and Li, Hasjim, Dhital, Godwin, and Gilbert (2011) with some modifications. Briefly, 6 mg of starch was incubated in 0.5 mL of protease solution (0.25 M tricine buffer, pH 7.5, 1.25 U protease (Sigma P5147)) at 37 °C for 30 min using a ThermoMixer with continuous shaking (350 rpm). The sample was centrifuged at 4000 *g* for 10 min. The precipitation was suspended in 0.5 mL of 0.45% sodium bisulfite solution (w/v) at 37 °C for 30 min using a ThermoMixer with continuous shaking (350 rpm). The sample was again centrifuged. The precipitation was suspended in 1.5 mL of DMSO solution including 0.5% LiBr (w/v) at 80 □ for overnight using a ThermoMixer with continuous shaking (350 rpm). The sample was centrifuged, and the supernatant was mixed with 4 volumes of absolute ethanol to precipitate the starch. The precipitation was washed with absolute ethanol, and then was dispersed using 0.9 mL of warm deionized water

and incubated in boiling water for 30 min. The sample was cooled to room temperature, added 0.1 mL of 0.1M acetate buffer (pH 3.5), 5 μL of 4% sodium azide solution (w/v), and 2.5 μL of isoamylase (Megazyme E-ISAMY), finally mixed and incubated at 37 °C for 3 h using a ThermoMixer with continuous shaking (350 rpm). The sample was added 0.1 mL of 0.1 M NaOH and freezed in liquid nitrogen followed by freeze-drying in freeze-dryer overnight. The dry starch powder (0.3 mg) was labeled with 3 μL of 8-amino-1,3,6-pyrenetrisulfonic acid (APTS) labeling dye (0.1 M APTS, 0.5 M sodium cyanoborohydride in 15% acetic acid) at 60 °C for 90 min using a ThermoMixer with continuous shaking (350 rpm). The labeled sample was diluted with 60 μL of deionized water and centrifuged. The 50 μL of supernatant was analyzed using a FACE (Beckman Coulter PA800, Fullerton, CA, USA) following the method of Cuevas, Daygon, Morell, Gilbert, and Fitzgerald (2010). The experiments were performed in duplicate.

2.4. Swelling power and water solubility determination

The swelling power and water solubility index of starch were determined with a small-scale test method according to the procedure of Konik-Rose et al. (2001) with some modifications. Thirty milligram of dry starch was weighed into a pre-weight micro-centrifuge tube (2 mL). The sample was well mixed with 1.5 mL of double-distilled water and then held in a water bath at 75, 85, or 95 °C for 30 min with regular gentle inversions (20 times over the first minute, then twice at 1.5, 2, 3, 4, 5, 7.5, 10, 15, 25 min). The sample was then cooled to room temperature in cool water. The tube was centrifuged at 8000 *g* for 20 min, and the supernatant was removed. The soluble carbohydrate in the supernatant was measured with anthrone-H_2SO_4 method. The swelling power was determined by measuring the amount of

original precipitate from the centrifugation and calculating the amount of water absorbed by the starch (percent weight increase) after subtraction of the amount of soluble carbohydrate. The water solubility was obtained by calculating the amount of soluble carbohydrate by the starch. The experiments were performed in triplicate.

2.5. Differential scanning calorimetry (DSC) analysis

Five milligram of starch was precisely weighed and mixed with 15 μL of deionized-distilled water. The mixture was sealed in an aluminum pan and equilibrated for 2 h at room temperature. The sample was then heated from room temperature to 130 °C at a rate of 10 °C/min using a DSC (200-F3, NETZSCH, Germany). The experiments were carried out in triplicate.

2.6. Hydrolysis degree determination

Starch was hydrolyzed by HCl, PPA, or AAG using the methods of Gao et al. (2014) and Li, Vasanthan, Hoover, and Rossnagel (2004) with some modifications. For HCl hydrolysis, 20 mg of starch was suspended in 2 mL of 2.2 M HCl and hydrolysis was conducted in a ThermoMixer at 35 °C with continuous shaking (1000 rpm) for 4 d. For PPA hydrolysis, 10 mg of starch was suspended in 2 mL of enzyme solution (0.1 M phosphate sodium buffer, pH 6.9, 25 mM NaCl, 5 mM $CaCl_2$, 0.02% NaN_3, 50 U PPA (Sigma A3176)) and hydrolysis was conducted in a ThermoMixer at 37 °C with continuous shaking (1000 rpm) for 12 h. For AAG hydrolysis, 10 mg of starch was suspended in 2 mL of enzyme solution (0.05 M acetate buffer, pH 4.5, 5 U AAG (Sigma A7095)) and hydrolysis was conducted in a ThermoMixer at 55 °C with continuous shaking (1000 rpm) for 12 h. After hydrolysis, starch slurry was quickly centrifuged (5000 *g*) at 4 °C for 5 min. The supernatant was used for measurement of the

194 soluble carbohydrates to quantify the amount of hydrolyzed starch using the anthrone-H_2SO_4
195 method. The hydrolysis degree was calculated as the amount (mg) of starch hydrolyzed per
196 100 mg of dry starch. The experiments were carried out in triplicate.

197 **2.7. *In vitro* digestion**

198 *In vitro* digestion of starch was analyzed following a method of Carciofi et al. (2012)
199 with some modifications. Ten milligram of starch was incubated in 2 mL of enzyme solution
200 (20 mM sodium phosphate buffer, pH 6.0, 6.7 mM NaCl, 0.01% NaN_3, 2.5 mM $CaCl_2$, 4 U
201 PPA (Sigma A3176), 4 U AAG (Megazyme E-AMGDF)). The digestion was conducted in a
202 ThermoMixer at 37 °C with continuous shaking (1000 rpm) for 20 and 120 min. Enzyme
203 treatment was terminated by adding 240 μL of 0.1 M HCl and 2 mL of 50% ethanol and
204 centrifuged (14000 *g*, 5 min). The glucose content in the supernatant was determined by the
205 D-Glucose (GOPOD Format) assay kit (Megazyme, K-GLUC). Starch nutritional fractions
206 based on the rate of hydrolysis were rapidly digestible starch (RDS, digested within 20 min),
207 slowly digestible starch (SDS, digested between 20 and 120 min) and resistant starch (RS,
208 undigested after 120 min). The experiments were performed in triplicate.

209 **2.8. Statistical analysis**

210 The data reported in all the tables were mean values and standard deviation. Analysis of
211 variance (ANOVA) using Tukey's test ($p < 0.05$) and Pearson's bivariate correlations were
212 performed with SPSS 19.0 Statistical Software Program. Dendrograms were obtained by
213 Minitab V. 16.0 software.

214 **3. Results and discussion**

215 **3.1. Amylopectin molecular structures of different-sized fractions of starch**

The chain length distribution of amylopectin as determined by FACE is shown in Fig. 1. The different-sized fractions of normal maize starch showed the same FACE chromatograms. But the markedly different FACE chromatograms could be observed in the different-sized fractions of high-amylose maize starch. Amylopectin branch-chains are usually classified by the degree of polymerization (DP) into the following types: A chain (DP 6−12), B1 chain (DP 13−24), B2 chain (DP 25−36), and B3+ chains (DP≥37) (Hanashiro, Abe, & Hizukuri, 1996). The average branch-chain length of amylopectin can be obtained by calculating the ratio of total glucose (DP 6−100 × their areas) to total areas of DP 6−100. The percentages of A, B1, B2 and B3+ chains and the average branch-chain length of amylopectin in native and different-sized fractions of normal and high-amylose maize starches are shown in Table 1. The chain length distribution and average branch-chain length of amylopectins of the different-sized fractions of normal maize starch had no difference, and were similar to those of the large-sized fraction of high-amylose starch. But the A and B1 chains of amylopectin significantly decreased and the B2 and B3+ chains and average branch-chain length of amylopectin significantly increased with the decrease of granule size among the different-sized fractions of high-amylose maize starch (Table 1). The present results were in agreement with our previous results of gel permeation chromatography that the amylopectin short branch-chain significantly decreased and amylopectin long branch-chain increased with the decrease of granule size in high-amylose maize starch, but they were similar among different-sized fractions of normal maize starch (Cai, Lin et al., 2014).

3.2. Swelling powers and water solubilities of different-sized fractions of starch

Swelling power and water solubility of starch were determined at 75, 85, and 95 °C

(Table 2). The swelling power and water solubility did not significantly change in different-sized fractions of normal maize starch at 75 and 85 °C, but significantly increased in small-sized fraction at 95 °C. For high-amylose maize starch, swelling power and water solubility markedly decreased with decrease of granule size (Table 2). The swelling power and solubility provide measures of the magnitude of interaction between starch chains within the amorphous and crystalline domains. The extent of this interaction is influenced by the amylose to amylopectin ratio, the characteristics of the amylose and amylopectin in terms of molecular weight/distribution, branching degree and branch length, and conformation (Kaur et al., 2007). Swelling power is positively correlated with amylopectin short branch-chains and negatively with amylopectin long branch-chains (Salman et al., 2009). Amylose restrains swelling and maintains the integrity of swollen granules, and the lipid-complexed amylose chains restrict both granular swelling and amylose leaching (Tester & Morrison, 1992). In the present study, the similar amylose content (Cai, Lin et al., 2014) and amylopectin branch-chain length distribution (Table 1) in different-sized fractions of normal maize starch resulted in the similar swelling power and water solubility, and the much higher amylose content (Cai, Lin et al., 2014) and amylopectin long branch-chains (Table 1) in small-sized fraction of high-amylose maize starch led to the significantly lower swelling power and water solubility than its counterpart medium- and large-sized fractions.

3.3. Thermal properties of different-sized fractions of starch

Thermal properties of native and different-sized fractions of normal and high-amylose maize starches were analyzed using DSC, and the DSC parameters are shown in Table 3. A similar gelatinization temperature and enthalpy were observed in different-sized fractions of

normal maize starch. Similar results have also been reported in normal maize and potato starch (Dhital et al., 2011). However, the gelatinization peak temperature increased and enthalpy value markedly decreased with decrease of granule size for high-amylose maize starch. Noda, Takahata, Sato, Ikoma, and Mochida (1996) postulate that the DSC parameters are influenced by the molecular architecture of the crystalline region, which corresponds to the distribution of amylopectin chain length distribution. The gelatinization temperature is positively correlated to the branch-chain length of amylopectin, longer chain length displaying higher gelatinization temperature (Shi & Seib, 1995). For high-amylose starch, the B-type crystalline results in higher gelatinization temperature than normal starch (Richardson, Jeffcoat, & Shi, 2000). The amylose double helices also require a high temperature and energy input to become disordered, which leads to a high gelatinization temperature (Shi, Capitani, Trzasko, & Jeffcoat, 1998). In the present study, the different variation in thermal properties of different-sized fractions of normal and high-amylose maize starches might be due to differences in the chain length distribution of amylopectin. The longer chains in small-sized fractions of high-amylose maize starch required a higher temperature to dissociate completely than that required for shorter double helices in medium- and large-sized fractions. Gelatinization enthalpy primarily reflects the loss of double helical order and decreases with amylose content increase (Matveev et al., 2001). In the present study, the lower enthalpy of the small-sized fraction of high-amylose maize starch suggested a less organized arrangements or lower stability of the crystals in them than in its counterpart medium- and larger-sized fractions (Singh & Kaur, 2004).

3.4. Hydrolysis degrees of different-sized fractions of starch

The applications of starch in food and nonfood industries require the disruption of starch granules. Acid hydrolysis is widely used to produce thin boiling starches for use in food, paper, textile, and other industries (Rohwer & Klem, 1984). Enzyme hydrolysis of starch is involved in many industrial processes, such as malting, fermentation, glucose syrup, and bioethanol production. The α-amylase is an endoamylase that cleaves the α-1,4-glycosidic bonds of the amylose or amylopectin chain at internal positions (endo) to yield products (oligosaccharides with varying lengths and branched oligosaccharides called limit dextrins) with an α-configuration. The amyloglucosidase is an exoamylase that catalyses the hydrolysis of both α-1,4 and α-1,6 glycosidic bonds at the branching point to release β-D-glucose residues of the polymer substrate (Tawil, Viksø-Nielsen, Rolland-Sabaté, Colonna, & Buléon, 2011; van der Maarel, van der Veen, Uitdehaag, Leemhuis, & Dijkhuizen, 2002). Therefore, it is very important to investigate the hydrolysis properties of acid, α-amylase and amyloglucosidase for starch applications. In the present study, native and different-sized fractions of normal and high-amylose maize starches were subjected to 4 days of HCl hydrolysis and 12 h of PPA and AAG hydrolysis (Table 4). The hydrolysis degree of normal maize starch slightly increased with decrease of granule size from 56.8 to 59.8% for HCl, from 86.2 to 87.6% for PPA, and from 72.7 to 77.9% for AAG. By contrast, the hydrolysis degree of high-amylose maize starch markedly decreased with decrease of granule size from 54.8 to 32.3% for HCl, from 81.8 to 40.0% for PPA, and from 73.8 to 37.5% for AAG. Susceptibility of starch to HCl, PPA and AAG attack is influenced by factors such as amylose content, crystalline structure, granule size and relative surface area, granule integrity, and porosity of granules (Blazek & Gilbert, 2010). The degree of native starch hydrolysis by

amylase or acid is inversely related to the amylose content (Li et al., 2004). The A-, B- and C-type starches show different susceptibilities to amylase hydrolysis. Generally, the B- or C-type starch shows more resistance to enzyme hydrolysis than the A-type starch (Tester, Karkalas, & Qi, 2004b). In the present study, different-sized fractions of normal maize starch had similar amylose content (Cai, Lin et al., 2014), amylopectin chain length distribution (Table 1), and crystalline structure (Cai, Lin et al., 2014), resulting in that they had slight variation in hydrolysis properties. Though they had different size, the apparent available surface area (as represented by granule size) was relatively unimportant due to the presence of surface pores and channels, therefore the difference in rate and extent of amylolysis between different-sized fractions of normal maize starch was not significant (Dhital et al., 2010, 2011). For high-amylose maize, the small-sized fraction of starch had significantly higher amylose content (Cai, Lin et al., 2014) and amylopectin long branch-chain and average banch-chain length and lower amylopectin short branch-chain than the large-sized fraction (Table 1). The proportion of B-type crystallinity increased and gelatinization enthalpy decreased with decrease of granule size in high-amylose maize starch (Table 3) (Cai, Lin et al., 2014). The above significant differences in molecular and crystalline structure led to the marked variation in hydrolysis properties of different-sized fractions of high-amylose maize starch.

3.5. *In vitro* digestion properties of different-sized fractions of starch

The *in vitro* digestion properties of starches are shown in Table 5. For normal maize, the starch granules were rapidly digested with decrease of granule size at initial 20 min of digestion, but after 2 h of digestion, the large-sized fraction was digested more extensively than the small-sized fraction, resulting in that small-sized fraction had higher RS content than

large-sized fraction. Similar results were also reported in normal triticale, wheat, and corn starches (Naguleswaran et al., 2012; Salman et al., 2009). At the initial stages, enzyme digestion is dependent mainly on contact between the enzyme and the surface of starch granules and, thus, the surface area of the granules is important in determining the initial attack on the granules by the enzyme. The larger relative surface area of small-size granules is consistent with their greater initial digestibility by enzymes compared to the large-size granules (Kim, Kong, Kim, & Lee, 2008; Salman et al., 2009). In addition, the higher digestion of small-sized fraction could be attributed to its weak association of double helices within the crystalline lamellae reflected by lesser gelatinization enthalpy (Table 3) than that of large-sized fraction (Kim et al., 2008; Naguleswaran, Vasanthan, Hoover, & Bressler, 2013). Surface pores and internal channels of granules are assumed to increase effective surface area for fast enzyme diffusion. However, the presence of minor components, such as proteins and lipids on granule surface and in channels largely block the binding sites of enzyme, thereby reducing the rate of digestion, especially in large-size granules which have numerous pores and channels (Naguleswaran et al., 2012; Naguleswaran, Li, Vasanthan, & Bressler, 2011). With the progress of digestion, the digestion is more rapid in large-size granules possibly due to the gradual release of protein and lipid from associated glucan molecules. The densely packed crystalline lamellae and higher concentration of protein and lipid in small-size granules may greatly reduce digestion rate (Naguleswaran et al., 2011, 2012), resulting in the higher RS content in small-sized fraction of normal maize starch than large-sized fraction.

For high-amylose maize, the starch granules were slowly digested with decrease of granule size at both 20 min and 2 h of digestion, resulting in that the RS content markedly

increased with decrease of granule size. This previous studies suggested that amylolysis of large- and small-size starch granules is closely related to granule morphology, composition, and structure at granular micro- and nano-levels, such as shape, size, pores, channels, amylose content, associated protein and lipid, degree of crystallinity, lamellae size, and ratio of amylopectin long and short chains (Dhital et al., 2010; Naguleswaran et al., 2011, 2012; Salman et al., 2009). The B-type crystallinity containing longer double helices derived from long branch-chains of amylopectin is more resistance to digestion than A-type crystallinity containing short branch-chains of amylopectin (Dhital et al., 2015). In rice starches with different particle size, morphology, thermal properties, and crystalline polymorph, the longer branch length of amylopectin which leads to the formation of more stable B-type double helical structure compared to its A-type counterpart is the major parameter, with other factors such as granule size, surface pores and interior channels having secondary role, in determining the rate of enzymatic hydrolysis of rice starch granules (Dhital et al., 2015). Though the relative surface area of starch granules increased with decrease of granule size, the significantly higher B-type crystallinity content, amylose content, lipid content (Cai, Lin et al., 2014) and amylopectin long branch-chain and average branch-chain length (Table 1) resulted in markedly lower RDS and SDS contents and higher RS content in small-sized fraction of high-amylose maize starch than in large-sized fraction.

3.6. Relationships between amylopectin molecular structures and functional properties of different-sized fractions of starch

Amylopectin molecular structures affect the functional properties of starch. In the present study, Pearson's bivariate correlations with amylopectin molecular structures and functional

properties were shown in Table 6. The swelling power is a measure of the water-holding capacity of starch after being heated in water, cooled, and centrifuged, while the water solubility reflects the degree of dissolution during the starch swelling procedure. The difference in swelling power and water solubility between the starches can be attributed to the interplay of the following factors: (1) amylose content (Sasaki & Matsuki, 1998), (2) lipid-complexed amylose chains (Tester & Morrison, 1992), (3) molar proportion of amylopectin short branch-chains (Shi & Seib, 1992), and (4) extent of interaction between starch chains within the amorphous and crystalline domains (Hoover & Manuel, 1996). In the present study, Pearson's bivariate correlation analysis showed that the swelling power (at 75, 85 and 95 °C) and water solubility (at 95 °C) were significantly negatively correlative with amylopectin long branch-chains (DP≥25) and average branch-chain length and positively correlative with amylopectin short branch-chains (DP 6−24).

For normal starch, the gelatinization temperature decreases with an increase in amylose content. But for high-amylose starch, the gelatinization temperature increases with an increase in amylose content (Matveev et al., 2001; Richardson et al., 2000). The high-amylose starch usually has B- or C-type crystallinity (Cheetham & Tao, 1998). The B-type crystallinity needs higher gelatinization temperature than A-type crystallinity (Richardson et al., 2000). In high-amylose starch, the amylose double helices also require high temperature and energy to disorder and therefore lead to a high gelatinization temperature (Shi et al., 1998). Gelatinization temperature has been considered as a parameter of crystalline perfection. The long branch-chains in amylopectin cause an increase in the stability of the double helix and induce a higher gelatinization temperature (Chung, Liu, Lee, & Wei, 2011). In the present

study, gelatinization temperature was positively correlated with amylopectin long branch-chains and average branch-chain length and negatively correlated with amylopectin short branch-chains, but the gelatinization enthalpy was negatively correlated with amylopectin long branch-chains and average branch-chain length and positively correlated with amylopectin short branch-chains.

Starch hydrolysis and digestibility are influenced by amylopectin branch chain length distribution (Carciofi et al., 2012; Man et al., 2012; Regina et al., 2006; Slade et al., 2012; Zhang, Ao, & Hamaker, 2008; Zhu et al., 2012). Srichuwong, Isono, Mishima, and Hisamatsu (2005) show that enzyme hydrolysis of raw starches from different botanical sources is positively and negatively correlated with the proportion of DP 8−12 and DP 13−26 of amylopectin, respectively. Chuang et al. (2011) show that RS content is positively correlated with average branch-chain length and the proportion of DP 13−24 of amylopectin, but negatively correlated with the proportion of DP 6−12 of amylopectin. The short double helices formed from amylopectin short branch-chains in the crystalline region cause weak points in starch crystalline structure, resulting in greater susceptibility to hydrolysis (Jane, Wong, & McPherson, 1997). Zhang et al. (2008) report a parabolic relationship between SDS content and the weight ratio of amylopectin short branch-chains (DP<13) to long branch-chains (DP≥13), indicating that amylopectin with a higher amount of either short or long branch-chains can produce relatively high amounts of SDS. In the present study, Pearson's bivariate correlation analysis showed a significantly negative correlation of HCl hydrolysis, PPA hydrolysis, AAG hydrolysis, and digestion with amylopectin long branch-chains and average branch-chain length and a positive correlation with amylopectin

short branch-chains.

To further determine characteristics associated with amylopectin molecular structure and functional properties, cluster dendrogram with average linkage correlation was constructed (Fig. 2). The right branch cluster group consisted of amylopectin long branch-chains, amylopectin average branch-chain length, peak and conclusion gelatinization temperatures, gelatinization temperature range, and RS. The peak and conclusion gelatinization temperatures, resistant starch, and the proportions of amylopectin long branch-chains (DP 25−36) had >95% similarity, suggesting strong correlation among these variables. This set had >91% similarity with amylopectin average branch-chain length and the proportions of amylopectin long branch-chains (DP≥37). The left branch cluster group contained amylopectin short branch-chains, swelling power, water solubility, RDS, SDS, gelatinization onset temperature and enthalpy, and hydrolysis of HCl, PPA and AAG. The swelling power, hydrolysis of HCl, PPA and AAG, and water solubility at 95 °C had >97% similarity, suggesting strong correlation among these variables. This set was influenced by the set of amylopectin short branch-chains and gelatinization enthalpy (>95% similarity level), and had 93.5% similarity with SDS. This analysis revealed that variation in amylopectin long branch-chains and average branch-chain length significantly influenced gelatinization temperature and RS, and amylopectin short branch-chains played substantial roles in starch swelling power, water solubility, gelatinization enthalpy, hydrolysis of HCl, PPA and AAG, and digestion.

3.7. Cluster analysis of native and different-sized fractions of normal and high-amylose maize starch

436 In order to compare the relationships between different-sized fractions of normal and
437 high-amylose maize starches, the hierarchical cluster was analyzed on the basis of similarities
438 and differences in amylopectin molecular structure and starch functional properties (Fig. 3).
439 The dendrogram consisted of two major clusters. The two clusters were separated by distance
440 of 17.35. One cluster contained native and different-sized fractions of normal maize starch
441 and large-sized fraction of high-amylose maize starch, while another cluster included native
442 and medium- and small-sized fractions of high-amylose maize starch. This indicated that the
443 large-sized fraction of high-amylose maize starch was similar to normal maize starch in
444 overall amylopectin molecular structure and functional properties. Our previous study also
445 showed that the large-sized fraction of high-amylose maize starch was similar to normal
446 maize starch in morphological structure, granule size, crystalline structure and relative
447 crystallinity, lamellar structure, and short- and long-range ordered structure (Cai, Lin et al.,
448 2014). It was apparent from the dendrogram that the two main clusters could even be further
449 separated into distinct, smaller subclusters that enabled better sorting of the samples
450 according to amylopectin molecular structures and function properties. The small-sized
451 fraction of high-amylose starch was separated from native and medium-sized fraction of
452 high-amylose starch by average distance of 9.04. The large-sized fraction of high-amylose
453 starch was separated from native and different-sized fractions of normal maize starch by
454 average distance of 5.27. The results indicated that different-sized fractions of high-amylose
455 maize starch had markedly different amylopectin molecular structures and functional
456 properties and those of normal maize starch had similar amylopectin molecular structures and
457 functional properties, which was in agreement with their structural properties (Cai, Lin et al.,

458 2014).

459 **4. Conclusion**

460 The different-sized fractions of normal maize starch showed similar amylopectin
461 molecular structures and functional properties, but those of high-amylose maize starch had
462 significantly different amylopectin molecular structures and functional properties. The
463 amylopectin short branch-chain, swelling power, water solubility, gelatinization enthalpy, and
464 hydrolysis and digestion degrees of high-amylose starch significantly decreased with decrease
465 of granule size, but amylopectin long branch-chain and average branch-chain length,
466 gelatinization peak temperature, and RS content increased. The swelling power, gelatinization
467 enthalpy, and hydrolysis and digestion degrees were positively relative with amylopectin short
468 branch-chain but negatively relative with amylopectin long branch-chain and average
469 branch-chain length. The gelatinization temperature and RS content were positively relative
470 with amylopectin long branch-chain and average branch-chain length, and negatively relative
471 with amylopectin short branch-chain. The native and different-sized fractions of normal and
472 high-amylose starches could be classified into two major clusters according to their
473 amylopectin molecular structures and functional properties by hierarchical cluster analysis.
474 The large-sized fraction of high-amylose starch was very relative with normal starch. This
475 study could provide important information for the applications of different-sized fractions of
476 high-amylose maize starch.

477 **Acknowledgments**

478 This study was financially supported by grants from the National Natural Science Foundation

of China (31270221), the Talent Project of Yangzhou University, the Innovation Program for Graduates of Jiangsu Province, and the Priority Academic Program Development of Jiangsu Higher Education Institutions.

References

Blazek, J., & Gilbert, E. P. (2010). Effect of enzymatic hydrolysis on native starch granule structure. *Biomacromolecules*, *11*, 3275–3289.

Cai, C., Huang, J., Zhao, L., Liu, Q., Zhang, C., & Wei, C. (2014). Heterogeneous structure and spatial distribution in endosperm of high-amylose rice starch granules with different morphologies. *Journal of Agricultural and Food Chemistry*, *62*, 10143–10152.

Cai, C., Lin, L., Man, J., Zhao, L., Wang, Z., & Wei, C. (2014). Different structural properties of high-amylose maize starch fractions varying in granule size. *Journal of Agricultural and Food Chemistry*, *62*, 11711–11721.

Cai, C., Zhao, L., Huang, J., Chen, Y., & Wei, C. (2014). Morphology, structure and gelatinization properties of heterogeneous starch granules from high-amylose maize. *Carbohydrate Polymers*, *102*, 606–614.

Carciofi, M., Blennow, A., Jensen, S. L., Shaik, S. S., Henriksen, A., Buléon, A., Holm, P. B., & Hebelstrup, K. H. (2012). Concerted suppression of all starch branching enzyme genes in barley produces amylose-only starch granules. *BMC Plant Biology*, *12*, 223.

Cheetham, N. W. H., & Tao, L. (1998). Variation in crystalline type with amylose content in maize starch granules: an X-ray powder diffraction study. *Carbohydrate Polymers*, *36*, 277–284.

Chung, H. J., Liu, Q., Lee, L., & Wei, D. Z. (2011). Relationship between the structure,

physicochemical properties and *in vitro* digestibility of rice starches with different amylose contents. *Food Hydrocolloids*, *25*, 968–975.

Cuevas, R. P., Daygon, V. D., Morell, M. K., Gilbert, R. G., & Fitzgerald, M. A. (2010). Using chain-length distributions to diagnose genetic diversity in starch biosynthesis. *Carbohydrate Polymers*, *81*, 120-127.

Dhital, S., Butardo, V. M., Jobling, S. A., & Gidley, M. J. (2015). Rice starch granule amylolysis - differentiating effects of particle size, morphology, thermal properties and crystalline polymorph. *Carbohydrate Polymers*, *115*, 305–316.

Dhital, S., Shrestha, A. K., & Gidley, M. J. (2010). Relationship between granule size and *in vitro* digestibility of maize and potato starches. *Carbohydrate Polymers*, *82*, 480–488.

Dhital, S., Shrestha, A. K., Hasjim, J., & Gidley, M. J. (2011). Physicochemical and structural properties of maize and potato starches as a function of granule size. *Journal of Agricultural and Food Chemistry*, *59*, 10151–10161.

Gao, H., Cai, J., Han, W., Huai, H., Chen, Y., & Wei, C. (2014). Comparison of starches isolated from three different *Trapa* species. *Food Hydrocolloids*, *37*, 174–181.

Hanashiro, I., Abe, J., & Hizukuri, S. (1996). A periodic distribution of the chain length of amylopectin as revealed by high-performance anion-exchange chromatography. *Carbohydrate Research*, *283*, 151–159.

Hoover, R., & Manuel, H. (1996). The effect of heat-moisture treatment on the structure and physicochemical properties of normal maize, waxy maize, dull waxy maize and amylomaize V starches. *Journal of Cereal Science*, *23*, 153–162.

Jane, J. L., Kasemsuwan, T., Leas, S., Zobel, H., & Robyt, J. F. (1994). Anthology of starch

granule morphology by scanning electron microscopy. *Starch*, *46*, 121−129.

Jane, J. L., Wong, K. S., & McPherson, A. E. (1997). Branch-structure difference in starches of A- and B-type X-ray patterns revealed by their Naegeli dextrins. *Carbohydrate Research*, *300*, 219–227.

Kaur, L., Singh, J., McCarthy, O. J., & Singh, H. (2007). Physico-chemical, rheological and structural properties of fractionated potato starches. *Journal of Food Engineering*, *82*, 383–394.

Kim, J. C., Kong, B. W., Kim, M. J., & Lee, S. H. (2008). Amylolytic hydrolysis of native starch granules affected by granule surface area. *Journal of Food Science*, *73*, C621–C624.

Konik-Rose, C. M., Moss, R., Rahman, S., Appels, R., Stoddard, F., & McMaster, G. (2001). Evaluation of the 40 mg swelling test for measuring starch functionality. *Starch*, *53*, 14–20.

Li, E., Hasjim, J., Dhital, S., Godwin, I. D., & Gilbert, R. G. (2011). Effect of a gibberellin-biosynthesis inhibitor treatment on the physicochemical properties of sorghum starch. *Journal of Cereal Science*, *53*, 328–334.

Li, J. H., Vasanthan, T., Hoover, R., & Rossnagel, B. G. (2004). Starch from hull-less barley: V. In-vitro susceptibility of waxy, normal, and high-amylose starches towards hydrolysis by alpha-amylases and amyloglucosidase. *Food Chemistry*, *84*, 621–632.

Li, W., Shan, Y., Xiao, X., Luo, Q., Zheng, J., Ouyang, S., & Zhang, G. (2013). Physicochemical properties of A- and B-starch granules isolated from hard red and soft red winter wheat. *Journal of Agricultural and Food Chemistry*, *61*, 6477–6484.

545 Lindeboom, N., Chang, P. R., & Tyler, R. T. (2004). Analytical, biochemical and
546 physicochemical aspects of starch granule size, with emphasis on small granule starch: a
547 review. *Starch*, *56*, 89–99.
548 Man, J., Yang, Y., Zhang, C., Zhou, X., Dong, Y., Zhang, F., Liu, Q., & Wei, C. (2012).
549 Structural changes of high-amylose rice starch residues following in vitro and in vivo
550 digestion. *Journal of Agricultural and Food Chemistry*, *60*, 9332–9341.
551 Man, J., Lin, L., Wang, Z., Wang, Y., Liu, Q., & Wei, C. (2014). Different structures of
552 heterogeneous starch granules from high-amylose rice. *Journal of Agricultural and Food*
553 *Chemistry*, *62*, 11254–11263.
554 Matveev, Y. I., van Soest, J. J. G., Nieman, C., Wasserman, L. A., Protserov, V. A.,
555 Ezernitskaja, M., & Yuryev, V. P. (2001). The relationship between thermodynamic and
556 structural properties of low and high amylose maize starches. *Carbohydrate Polymers*,
557 *44*, 151–160.
558 Naguleswaran, S., Li, J., Vasanthan, T., & Bressler, D. (2011). Distribution of granule
559 channels, protein, and phospholipid in triticale and corn starches as revealed by confocal
560 laser scanning microscopy. *Cereal Chemistry*, *88*, 87–94.
561 Naguleswaran, S., Li, J., Vasanthan, T., Bressler, D., & Hoover, R. (2012). Amylolysis of
562 large and small granules of native triticale, wheat and corn starches using a mixture of
563 α-amylase and glucoamylase. *Carbohydrate Polymers*, *88*, 864–874.
564 Naguleswaran, S., Vasanthan, T., Hoover, R., & Bressler D. (2013). The susceptibility of
565 large and small granules of waxy, normal and high-amylose genotypes of barley and
566 corn starches toward amylolysis at sub-gelatinization temperatures. *Food Research*

International, *51*, 771–782.

Noda, T., Takahata, Y., Sato, T., Ikoma, H., & Mochida, H. (1996). Physicochemical properties of starches from purple and orange fleshed sweet potato roots at two levels of fertilizer. *Starch*, *48*, 395–399.

Regina, A., Bird, A., Topping, D., Bowden, S., Freeman, J., Barsby, T., Kosar-Hashemi, B., Li, Z., Rahman, S., & Morell, M. (2006). High-amylose wheat generated by RNA interference improves indices of large-bowel health in rats. *Proceedings of the National Academy of Sciences of the United States of America*, *103*, 3546−3551.

Richardson, P. H., Jeffcoat, R., & Shi, Y. C. (2000). High-amylose starches: From biosynthesis to their use as food ingredients. *Materials Research Society Bulletin*, *25(12)*, 20–24.

Rohwer, R. G., & Klem, R. E. (1984). Acid-modified starch: production and used. In J. N. Bemiller, & E. F. Paschall (Eds.), *Starch: Chemistry and technology* (pp. 529–541). Orlando, FL: Academic press.

Salman, H., Blazek, J., Lopez-Rubio, A., Gilbert, E. P., Hanley, T., & Copeland, L. (2009). Structure–function relationships in A and B granules from wheat starches of similar amylose content. *Carbohydrate Polymers*, *75*, 420–427.

Sasaki, T., & Matsuki, J. (1998). Effect of wheat structure on swelling power. *Cereal Chemistry*, *75*, 525–529.

Shi, Y. C., & Seib, P. A. (1992). The structure of four waxy starches related to gelatinization and retrogradation. *Carbohydrate Research*, *227*, 131–145.

Shi, Y. C., & Seib, P. A. (1995). Fine structure of maize starches from four wx-containing

genotypes of the W64A inbred line in relation to gelatinization and retrogradation. *Carbohydrate Polymers*, *26*, 141–147.

Shi, Y. C., Capitani, T., Trzasko, P., & Jeffcoat, R. (1998). Molecular structure of a low-amylopectin starch and other high-amylose maize starches. *Journal of Cereal Science*, *27*, 289–299.

Singh, N., & Kaur, L. (2004). Morphological, thermal, rheological and retrogradation properties of potato starch fractions varying in granule size. *Journal of the Science of Food and Agriculture*, *84*, 1241–1252.

Slade, A. J., McGuire, C., Loeffler, D., Mullenberg, J., Skinner, W., Fazio, G., Holm, A., Brandt, K. M., Steine, M. N., Goodstal, J. F., & Knauf, V. (2012). Development of high amylose wheat through TILLING. *BMC Plant Biology*, *12*, 69.

Srichuwong, S., Isono, N., Mishima, T., & Hisamatsu, M. (2005). Structure of lintnerized starch is related to X-ray diffraction pattern and susceptibility to acid and enzyme hydrolysis of starch granule. *International Journal of Biological Macromolecules*, *37*, 115–121.

Takeda, Y., Takeda, C., Mizukami, H., & Hanashiro, I. (1999). Structures of large, medium and small starch granules of barley grain. *Carbohydrate Polymers*, *38*, 109–114.

Tang, H., Ando, H., Watanabe, K., Takeda, Y., & Mitsunaga, T. (2001). Physicochemical properties and structure of large, medium and small granule starches in fractions of normal barley endosperm. *Carbohydrate Research*, *330*, 241–248.

Tawil, G., Viksø-Nielsen, A., Rolland-Sabaté, A., Colonna, P., & Buléon, A. (2011). In depth study of a new highly efficient raw starch hydrolyzing a-amylase from *Rhizomucor* sp.

Biomacromolecules, *12*, 34–42.

Tester, R. F., & Morrison, W. R. (1992). Swelling and gelatinization of cereal starches. III. some properties of waxy and normal nonwaxy barley starches. *Cereal Chemistry*, *69*, 654–658.

Tester, R. F., Karkalas, J., & Qi, X. (2004a). Starch composition, fine structure and architecture. *Journal of Cereal Science*, *39*, 151–165.

Tester, R. F., Karkalas, J., & Qi, X. (2004b). Starch structure and digestibility enzyme-substrate relationship. *World's Poultry Science Journal*, *60*, 186–195.

Tran, T. T. B., Shelat, K. J., Tang, D., Li, E., Gilbert, R. G., & Hasjim, J. (2011). Milling of rice grains. The degradation on three structural levels of starch in rice flour can be independently controlled during grinding. *Journal of Agricultural and Food Chemistry*, *59*, 3964–3973.

van der Maarel, M. J. E. C., van der Veen, B., Uitdehaag, J. C. M., Leemhuis, H., & Dijkhuizen, L. (2002). Properties and applications of starch-converting enzymes of the a-amylase family. *Journal of Biotechnology*, *49*, 137–155.

Zhang, G., Ao, Z., & Hamaker, B. R. (2008). Nutritional property of endosperm starches from maize mutants: a parabolic relationship between slowly digestible starch and amylopectin fine structure. *Journal of Agricultural and Food Chemistry*, *56*, 4686–4694.

Zhu, L. J., Gu, M. H., Meng, X. L., Cheung, S. C. K. , Yu, H. X., Huang, J., Sun, Y., Shi, Y. C., & Liu, Q. Q. (2012). High-amylose rice improves indices of animal health in normal and diabetic rats. *Plant Biotechnology Journal*, *10*, 353–362.

Tables and figures

Table 1. Amylopectin molecular structures of native and different-sized fractions of normal and high-amylose maize starches [a]

Fraction	DP 6−12 (%)	DP 13−24 (%)	DP 25−36 (%)	DP ≥37 (%)	ABL (DP) [b]
Normal maize (NM) native	22.4±1.1c	49.2±0.2c	13.6±0.4a	14.9±0.9a	22.8±0.5a
NM large-sized	22.7±0.3c	49.2±0.6c	13.8±0.1a	14.3±1.0a	22.5±0.5a
NM medium-sized	21.9±1.5c	48.6±0.0c	13.4±0.6a	16.0±0.9a	23.4±0.6a
NM small-sized	21.9±0.3c	48.8±0.4c	13.4±0.1a	15.9±0.2a	23.3±0.1a
High-amylose maize (HM) native	18.5±0.4b	45.3±0.6b	14.4±0.1a	21.8±1.0b	26.9±0.6b
HM large-sized	21.2±0.4bc	48.7±0.2c	14.1±0.3a	16.1±0.1a	23.4±0.0a
HM medium-sized	19.9±0.4bc	48.5±0.1c	14.5±0.1a	17.1±0.4a	24.1±0.3a
HM small-sized	12.4±0.9a	37.4±0.8a	15.6±0.4b	34.6±1.2c	34.7±0.7c

[a] Data are means ± standard deviations, n = 2. Values in the same column with different letters are significantly different ($p < 0.05$).

[b] ABL: average branch-chain length of amylopectin.

Table 2. Swelling powers and water solubilities of native and different-sized fractions of normal and high-amylose maize starches [a]

Fraction	Swelling power (g/g)			Water solubility (%)		
	75 ºC	85 ºC	95 ºC	75 ºC	85 ºC	95 ºC
Normal maize (NM) native	11.6±0.1de	13.7±0.1e	17.0±0.1f	4.7±0.1c	8.8±0.1cd	15.5±0.3d
NM large-sized	11.7±0.0def	13.8±0.2e	15.3±0.1d	5.1±0.1d	9.9±0.3e	14.5±0.3c
NM medium-sized	11.9±0.1f	13.8±0.1e	15.9±0.1e	3.9±0.1b	8.4±0.2c	14.5±0.1c
NM small-sized	11.5±0.1d	13.6±0.1e	17.5±0.2g	4.5±0.1c	8.5±0.2c	16.0±0.2d
High-amylose maize (HM) native	7.6±0.0b	9.4±0.1b	12.3±0.0b	5.5±0.1e	9.1±0.1d	12.0±0.2b
HM large-sized	11.8±0.2ef	12.6±0.1d	16.1±0.2e	7.8±0.1f	11.6±0.1f	14.2±0.3c
HM medium-sized	9.5±0.2c	10.0±0.0c	13.8±0.2c	4.0±0.1b	7.3±0.1b	12.2±0.1b
HM small-sized	5.7±0.0a	6.9±0.0a	8.3±0.0a	3.4±0.1a	6.6±0.0a	10.6±0.2a

[a] Data are means ± standard deviations, n = 3. Values in the same column with different letters are significantly different ($p < 0.05$).

Table 3. Thermal properties of native and different-sized fractions of normal and high-amylose maize starches [a]

Fraction	T_o (°C) [b]	T_p (°C) [b]	T_c (°C) [b]	ΔT (°C) [b]	ΔH (J/g) [b]
Normal maize (NM) native	62.6±0.2bc	67.9±0.1a	73.5±0.3a	10.9±0.4a	10.2±0.4cd
NM large-sized	63.0±0.3cd	67.8±0.2a	73.3±0.3a	10.3±0.1a	10.4±0.8cd
NM medium-sized	63.4±0.1de	68.2±0.2a	73.7±0.3a	10.3±0.4a	10.8±0.4d
NM small-sized	61.9±0.3a	68.2±0.2a	74.0±0.2a	12.1±0.3b	9.5±0.7c
High-amylose maize (HM) native	64.3±0.1f	69.3±0.3bc	74.8±0.0b	10.5±0.1a	7.4±0.5b
HM large-sized	63.7±0.2ef	69.0±0.2b	74.8±0.4b	11.1±0.5ab	10.2±0.2cd
HM medium-sized	64.1±0.1f	69.8±0.3c	75.3±0.3bc	11.1±0.2ab	7.6±0.2b
HM small-sized	62.1±0.5ab	70.9±0.1d	75.9±0.5c	13.8±0.9c	2.6±0.2a

[a] Data are means ± standard deviations, n = 3. Values in the same column with different letters are significantly different ($p < 0.05$).

[b] T_o: onset temperature; T_p: peak temperature; T_c: conclusion temperature; ΔT: gelatinization temperature range (Tc-To); ΔH: gelatinization enthalpy.

Table 4. Hydrolysis degrees of native and different-sized fractions of normal and high-amylose maize starches [a]

Fraction	Hydrolysis degree by HCl for 4 d (%)	Hydrolysis degree by PPA for 12h (%)	Hydrolysis degree by AAG for 12h (%)
Normal maize (NM) native	59.5±0.2e	86.8±0.5d	74.9±1.3de
NM large-sized	56.8±0.5d	86.2±0.1d	72.7±1.1d
NM medium-sized	58.9±0.7e	87.4±0.4d	77.3±0.3ef
NM small-sized	59.8±0.4e	87.6±0.2d	77.9±1.1f
High-amylose maize (HM) native	44.5±0.4b	61.0±0.4b	61.5±0.3c
HM large-sized	54.8±0.8c	81.8±1.8c	73.8±1.1d
HM medium-sized	44.7±0.9b	58.8±0.4b	56.8±0.0b
HM small-sized	32.3±0.4a	40.0±0.7a	37.5±0.2a

[a] Data are means ± standard deviations, n = 3. Values in the same column with different letters are significantly different ($p < 0.05$).

Table 5. Digestion properties of native and different-sized fractions of normal and high-amylose maize starches [a]

Fraction	RDS (%) [b]	SDS (%) [b]	RS (%) [b]
Normal maize (NM) native	14.1±0.4e	40.0±0.0e	45.9±0.4ab
NM large-sized	10.2±0.5c	45.5±0.1f	44.3±0.3a
NM medium-sized	11.4±0.1d	40.7±1.2e	47.9±1.3b
NM small-sized	15.3±0.5f	36.3±0.3d	48.4±0.8b
High-amylose maize (HM) native	8.5±0.0b	24.6±0.4c	66.9±0.4d
HM large-sized	9.5±0.2bc	38.7±1.1e	51.8±1.4c
HM medium-sized	9.1±0.2b	21.1±0.0b	69.9±0.2e
HM small-sized	6.8±0.2a	17.9±0.5a	75.3±0.7f

[a] Data are means ± standard deviations, n = 3. Values in the same column with different letters are significantly different ($p < 0.05$).

[b] RDS: rapidly digestible starch; RS: resistant starch; SDS: slowly digestible starch.

Table 6. Correlation coefficients between amylopectin molecular structures and functional properties of native and different-sized fractions of normal and high-amylose maize starches [a]

	SP75	SP85	SP95	WS75	WS85	WS95	*To*	*Tp*	*Tc*	*ΔT*	*ΔH*	HCl	PPA	AAG	RDS	SDS	RS
DP 6-12	0.945**	0.942**	0.952**	0.352	0.585	0.872**	0.150	−0.921**	−0.848**	−0.780*	0.978**	0.946**	0.934**	0.947**	0.710*	0.837**	−0.867**
DP 13-24	0.906**	0.865**	0.927**	0.376	0.558	0.791*	0.279	−0.825*	−0.729*	−0.790*	0.943**	0.876**	0.854**	0.891**	0.644	0.722*	−0.754*
DP 25-36	−0.908**	−0.956**	−0.946**	−0.200	−0.460	−0.932**	0.037	0.947**	0.890**	0.667	−0.938**	−0.977**	−0.961**	−0.975**	−0.838**	−0.840**	0.899**
DP ≥37	−0.921**	−0.890**	−0.932**	−0.376	−0.576	−0.812*	−0.248	0.857**	0.769*	0.796*	−0.957**	−0.896**	−0.878**	−0.906**	−0.653	−0.763*	0.791*
ABL	−0.921**	−0.890**	−0.934**	−0.382	−0.579	−0.813*	−0.250	0.854**	0.764*	0.794*	−0.958**	−0.897**	−0.879**	−0.909**	−0.654	−0.761*	0.790*

[a]*, significant at $p < 0.05$; **, significant at $p < 0.01$.

ABL: average branch-chain length of amylopectin; DP 6−12, DP 13−24, DP 25−36, and DP≥37: proportion of amylopectin branch-chain (DP 6−12, DP 13−24, DP 25−36, and DP ≥37); HCl, PPA, and AAG: hydrolysis degree of HCl for 4 d, PPA for 12h, and AAG for 12 h; RDS: rapidly digestible starch; RS: resistant starch; SDS: slowly digestible starch; SP75, SP85, and SP95: swelling power at 75, 85, and 95 ºC; *To*, *Tp*, *Tc*: onset, peak, and conclusion gelatinization temperature; WS75, WS85, and WS95: water solubility at 75, 85, and 95 ºC; *ΔH*: gelatinization enthalpy; *ΔT*: gelatinization temperature range.

Figure captions

Fig. 1. FACE chromatogram of amylopectin from normal (A) and high-amylose (B) maize starches. NS, NS-L, NS-M, and NS-S: native and large-, medium-, and small-sized fractions of normal maize starch; HS, HS-L, HS-M, and HS-S: native and large-, medium-, and small-sized fractions of high-amylose maize starch.

Fig. 2. Average linkage dendrogram depicting relationships between amylopectin molecular structures and functional properties of native and different-sized fractions of normal and high-amylose maize starches. ABL: average branch-chain length of amylopectin; DP 6−12, DP 13−24, DP 25−36, and DP≥37: proportion of amylopectin branch-chain (DP 6−12, DP 13−24, DP 25−36, and DP ≥37); HCl, PPA, and AAG: hydrolysis degree of HCl for 4 d, PPA for 12h, and AAG for 12 h; RDS: rapidly digestible starch; RS: resistant starch; SDS: slowly digestible starch; SP75, SP85, and SP95: swelling power at 75, 85, and 95 ºC; *To*, *Tp*, *Tc*: onset, peak, and conclusion gelatinization temperature; WS75, WS85, and WS95: water solubility at 75, 85, and 95 ºC; ΔH: gelatinization enthalpy; ΔT: gelatinization temperature range.

Fig. 3. Ward linkage dendrogram generated by hierarchical cluster analysis of native and different-sized fractions of normal and high-amylose maize starches on basis of their amylopectin molecular structures and functional properties.

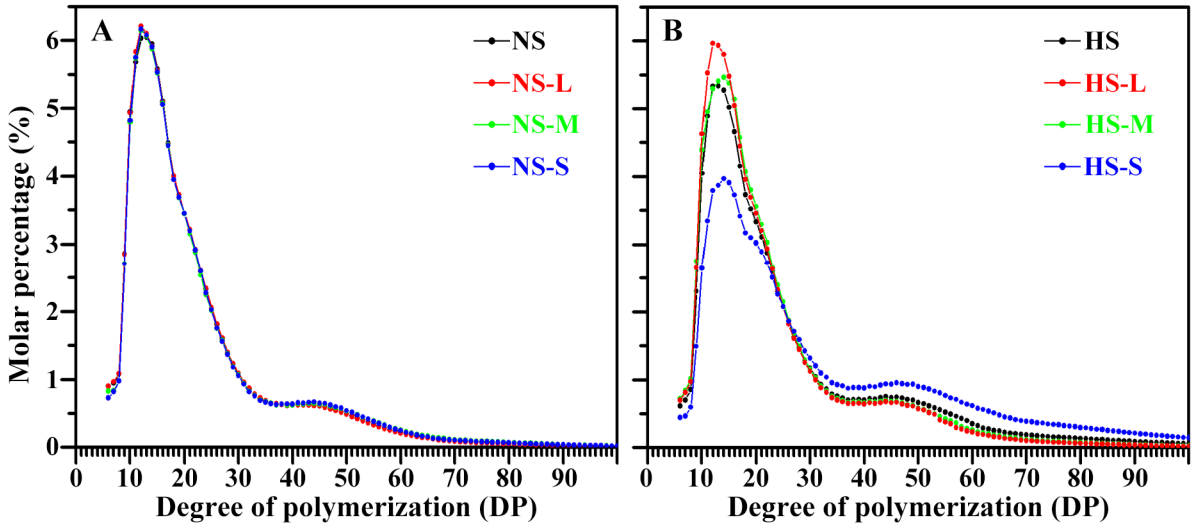

Fig. 1. FACE chromatogram of amylopectin from normal (A) and high-amylose (B) maize starches. NS, NS-L, NS-M, and NS-S: native and large-, medium-, and small-sized fractions of normal maize starch; HS, HS-L, HS-M, and HS-S: native and large-, medium-, and small-sized fractions of high-amylose maize starch.

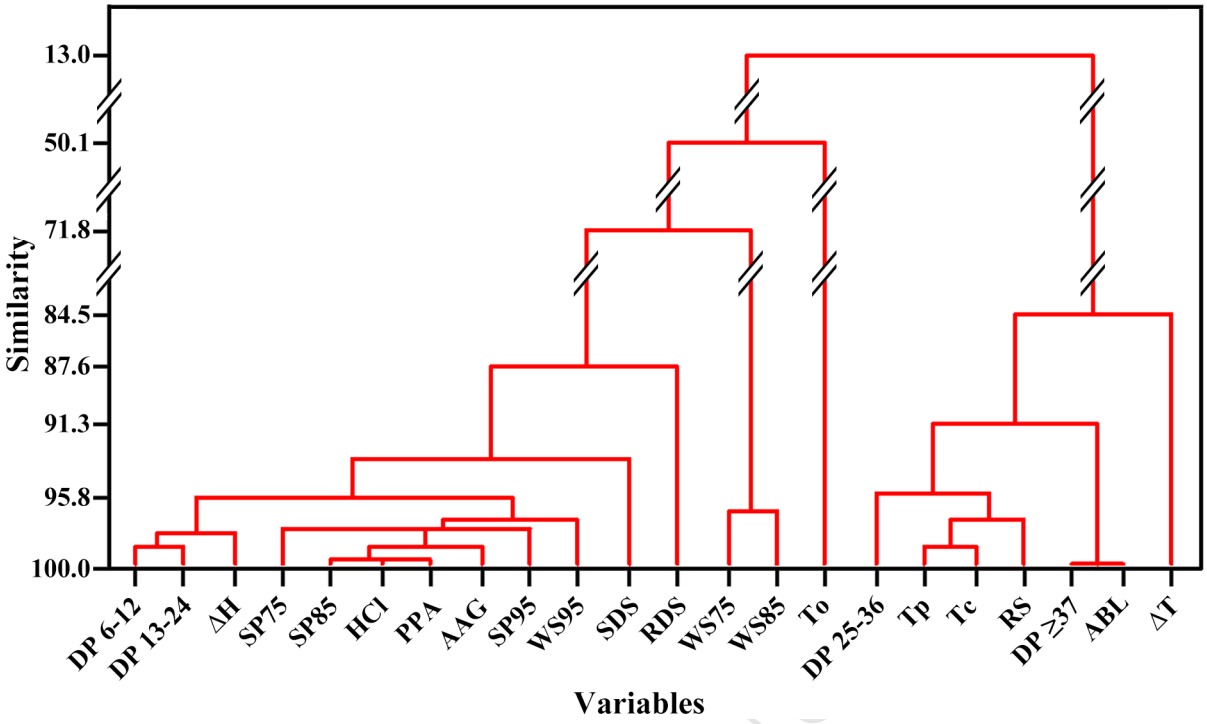

Fig. 2. Average linkage dendrogram depicting relationships between amylopectin molecular structures and functional properties of native and different-sized fractions of normal and high-amylose maize starches. ABL: average branch-chain length of amylopectin; DP 6−12, DP 13−24, DP 25−36, and DP≥37: proportion of amylopectin branch-chain (DP 6−12, DP 13−24, DP 25−36, and DP ≥37); HCl, PPA, and AAG: hydrolysis degree of HCl for 4 d, PPA for 12h, and AAG for 12 h; RDS: rapidly digestible starch; RS: resistant starch; SDS: slowly digestible starch; SP75, SP85, and SP95: swelling power at 75, 85, and 95 ºC; *To*, *Tp*, *Tc*: onset, peak, and conclusion gelatinization temperature; WS75, WS85, and WS95: water solubility at 75, 85, and 95 ºC; *ΔH*: gelatinization enthalpy; *ΔT*: gelatinization temperature range.

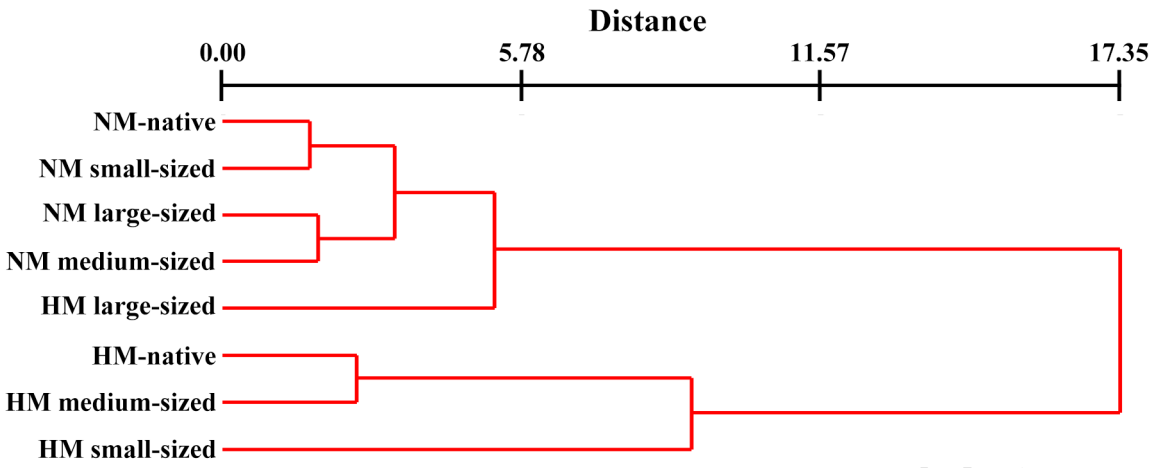

Fig. 3. Ward linkage dendrogram generated by hierarchical cluster analysis of native and different-sized fractions of normal and high-amylose maize starches on basis of their amylopectin molecular structures and functional properties.

- Different-sized fractions of normal and high-amylose maize starches were separated.
- Their amylopectin molecular structures and functional properties were investigated.
- The relationships between structures and functional properties were analyzed.
- Cluster dendrogram between structures and functional properties was constructed.
- Large-sized fraction of high-amylose starch was very relative with normal starch.